Pure & Appl. Chem., Vol. 59, No. 10, pp. 1307–1326, 1987.
Printed in Great Britain.

Determination of vibrational potential energy surfaces from Raman and infrared spectra

J. Laane

Department of Chemistry, Texas A&M University, College Station, TX 77843 U.S.A.

Abstract - Raman spectra, far-infrared spectra, and mid-infrared combination band data can be used to determine one-, two-, or three-dimensional potential energy functions which govern conformational changes in small ring molecules. The methods for such analyses are presented along with a brief history of the important contributions to this area. Recent studies on four-, five-, and six-membered rings and on some bicyclic systems are described. Potential difficulties in the calculation of high energy barriers are discussed along with how molecular mechanics calculations can be used to help estimate such barriers. The types of molecules for which the potential energy surfaces have been determined include cyclobutane, cyclopentane, cyclopentene, cyclohexane, cyclohexene, the cyclohexadienes, and the analogous ring systems containing oxygen, sulfur, silicon, nitrogen, phosphorous, or other heteroatoms. A number of bicyclohexanes, bicycloheptenes, and other bicyclic molecules have also been investigated.

INTRODUCTION

Conformational changes in molecules often occur via a vibrational pathway which can be investigated spectroscopically. For example, the inversion of ammonia or the internal rotation of ethane represent cases where the molecules must encounter energy barriers before converting to different (but energetically equivalent) structures. Similarly, small ring molecules such as cyclopentene, shown in Fig. 1, undergo ring-puckering vibrations which convert the molecule from one minimum energy conformation to another. For cyclopentene, and many other ring molecules, a puckered conformation lies lower in energy than one with a planar ring configuration. Hence, a barrier to planarity exists, and a double-minimum potential energy function results when the conformational changes are described in terms of a ring-puckering coordinate (defined for a four-membered ring in Fig. 2). As an example, Fig. 3 shows the one-dimensional potential energy function for silacyclobutane (ref. 1), which was one of the first molecules for which an accurate ring-puckering potential was determined from far-infrared data. This potential function was confirmed by the observation of the Raman spectrum (ref. 2), which is shown in Fig. 4. It should be noted that, in general, the infrared transitions correspond to single quantum jumps (the transitions shown on the left hand side of Fig. 3) whereas the Raman transition are double quantum jumps (right hand side of the figure). The combination of infrared and Raman spectra, when analyzed by quantum mechanical methods, thus serves as a powerful method for elucidating the energy changes associated with conformational processes.

Fig. 1. The ring-puckering vibration of cyclopentene.

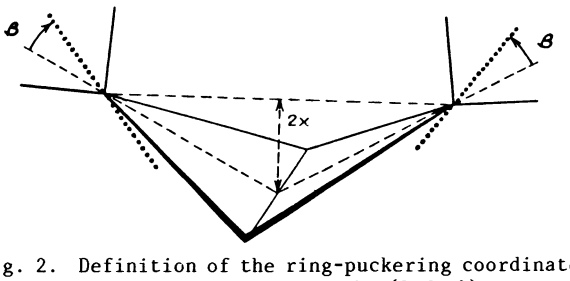

Fig. 2. Definition of the ring-puckering coordinate for a four-membered ring molecule (Ref. 8).

TABLE I. A historical summary of vibrational potential energy studies

Year	Development	Principal Authors	References
1930	Calculation of quartic oscillator eigenvalues	E. M. Milne	3
1945	Prediction of quartic oscillator levels for cyclobutane	R. P. Bell	4
1947	Prediction of free pseudorotation for cyclopentane	K. S. Pitzer	5
1960	First far-infrared spectrum of trimethylene oxide (TMO)	A. Danti, W. J. Lafferty, R. C. Lord	29
1960	First microwave spectrum of TMO	W. D. Gwinn	30
1965	Far-infrared spectrum of the pseudorotation of tetrahydrofuran	Lafferty, H. L. Strauss	31
1966-68	Potential energy functions for TMO, trimethylene sulfide, and silacyclobutane	Gwinn, Strauss; Laane, Lord	1,32,33
1966-67	Development of computer programs for calculating ring-puckering energy levels	Gwinn, Strauss; Laane, Lord; T. Ueda, T. Shimanouchi	16,17,32
1967	Potential functions for "pseudo-four-membered" rings	Laane, Lord; Ueda, Shimanouchi	16,17
1968	Observation of pseudorotational combination bands of cyclopentane	J. R. Durig, D. W. Wertz	27
1969	Observation of hindered pseudorotation	L. A. Carreira, Lord; Durig; Laane; Wertz; Strauss; Gwinn	34-39
1969	Asymmetric potential energy functions	Carreira, Lord	40
1969-74	Ring-puckering of bicyclic molecules and six-membered rings (pseudo-four-membered rings)	Laane, Lord, T. B. Malloy, Carreira	40-43
1970	Low-frequency Raman spectra of cyclobutane	R. J. Capwell, F. A. Miller; J.M.R. Stone, I.M. Mills	6,7
1972	Two-dimensional potential energy surfaces	Ikeda, Lord; Carreira, W. Person, I. M. Mills	21,45,46
1972	Improved reduced mass calculations	Malloy	47
1970-80	Potential functions determined for many molecules	Lord; Durig; Laane; Carreira; Malloy; Strauss; Wieser	Many
1982	Improved methods for kinetic and potential energy calculations	Laane, M. Harthcock	10,11,13 24,25
1982	Three-dimensional potential energy surface for DSCB	Laane, P. M. Killough, R. M. Irwin	13
1983	Asymmetric two-dimensional potential energy surface	Harthcock, Laane	24

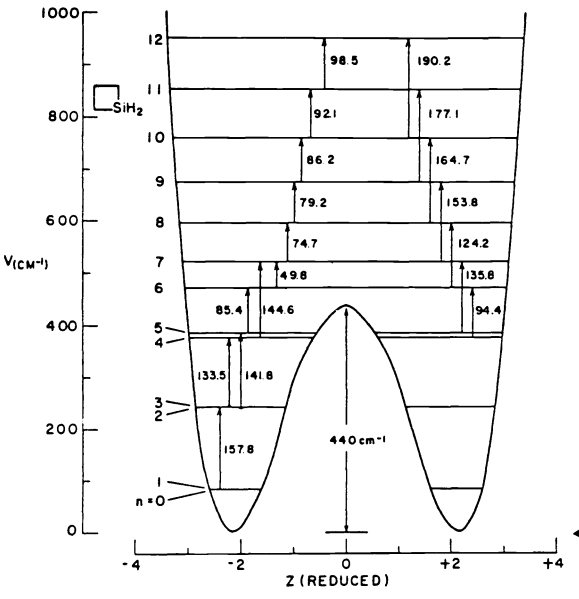

Fig. 3. Ring-puckering potential energy function for silacyclobutane (Ref. 1).

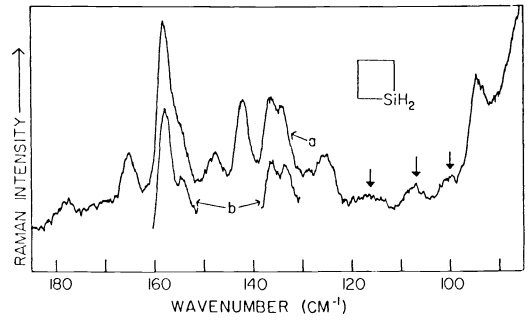

Fig. 4. Raman spectrum of silacyclobutane (Ref. 2).

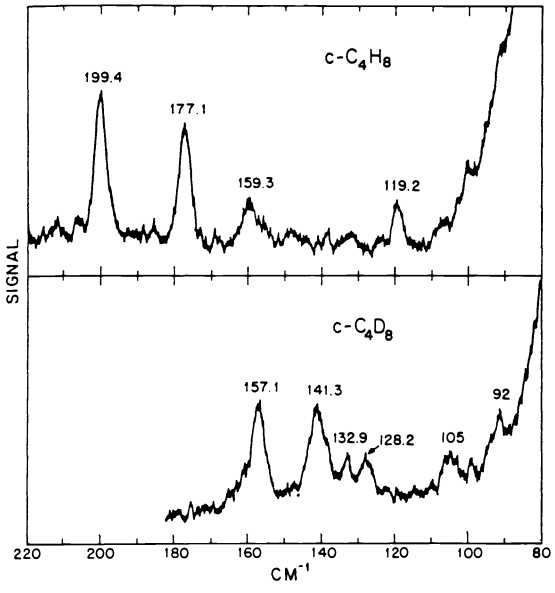

Fig. 5. Raman spectrum of cyclobutane (ref. 6).

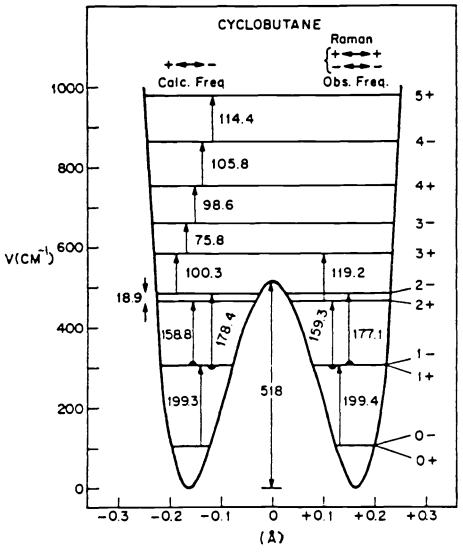

Fig. 6. Ring-puckering potential energy function of cyclobutane (ref. 6).

HISTORICAL

Table I presents a brief historical account (from the perspective of the author) of the major developments in the study of these types of potential energy functions. Milne's evaluation of quartic oscillator eigenfunctions (ref. 3) in 1930 followed by Bell's prediction (ref. 4) in 1945 that the puckering vibration of four-membered rings should be governed by quartic oscillator functions paved the way for the spectroscopic studies beginning in 1960. Similarly, the 1947 theoretical work on pseudorotation presented by Pitzer and co-workers (ref. 5) provided the groundwork for experimental studies on saturated five-membered rings in the next decade. Advances in instrumentation, including the development of FT-IR and laser Raman spectrophotometers, coupled with improved computational methods, have allowed potential energy studies to reach a much higher level of sophistication today.

The 1970 studies by Capwell and Miller (ref. 6) and Stone and Mills (ref. 7) on cyclobutane represented the first investigations of ring puckering by Raman spectroscopy. These studies were especially significant in that the ring-puckering vibration of this molecule is infrared inactive. Figure 5 shows the Raman spectrum and Fig. 6 the corresponding ring-puckering potential function for this molecule.

1,3-DISILACYCLOBUTANE (DSCB): A REPRESENTATIVE STUDY

In 1977 we published our preparation and spectroscopic study of 1,3-disilacyclobutane (ref. 8), $\overbrace{CH_2SiH_2CH_2SiH_2}$. Our efforts in synthesizing this molecule proved to be most worthwhile in that both the infrared and Raman spectra of the molecule are extremely rich with information. The analyses of the spectra of DSCB will be examined in some detail as a representative study.

Figure 7 and Fig. 8 show the far-infrared and Raman spectra of DSCB, respectively. The assignments of the spectra are facilitated by the use of Laane's tables (ref. 9), which present eigenvalues for mixed quartic/quadratic potential functions in reduced (undimensioned) form. The dimensioned potential

$$V = ax^4 + bx^2, \tag{1}$$

where x is the ring-puckering coordinate as defined in Fig. 3, is transformed to reduced coordinates using the expressions

$$Z = (2\mu/\hbar^2)^{1/6} a^{1/6} x \tag{2}$$

$$B = (2\mu/\hbar^2)^{1/3} a^{-2/3} b \tag{3}$$

$$\lambda = (2\mu/\hbar^2)^{2/3} a^{-1/3} E \tag{4}$$

and

$$A = (\hbar^2/2\mu)^{2/3} a^{1/3}. \tag{5}$$

Then the reduced potential, which facilitates computation, has the form

$$V = A\,(Z^4 + BZ^2), \tag{6}$$

where Z is the dimensionless coordinate related to x by Eq. (2). The eigenvalues λ for the potential in Eq. (6) have been tabulated (ref. 9) and their variation with B is presented in Fig. 9. For B=0 the levels are those of a pure quartic oscillator, whereas for very large B values harmonic oscillator levels are approached. When B is negative, a double minimum potential function with a barrier of $B^2/4$ results. The barrier is also shown in Fig. 9. The complexity of the spectra for such systems can be appreciated from Fig. 10, which shows the eigenvalue differences (proportional to frequencies) as a function of B. The reduced parameters which best fit the infrared and Raman data for DSCB are A = 15.19 cm^{-1} and B = -4.80. (Note that A serves as a scaling factor for the eigenvalues, i.e. $E = A\lambda$).

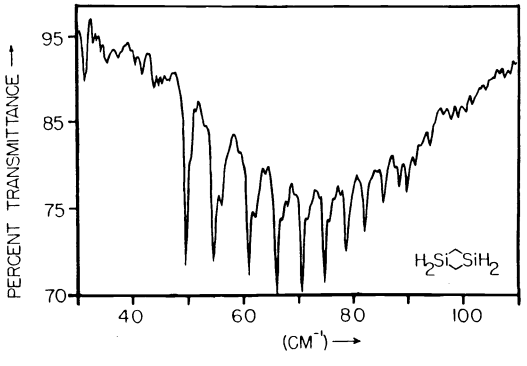

Fig. 7. Far-infrared spectrum of 1,3-disilacyclobutane (ref. 8).

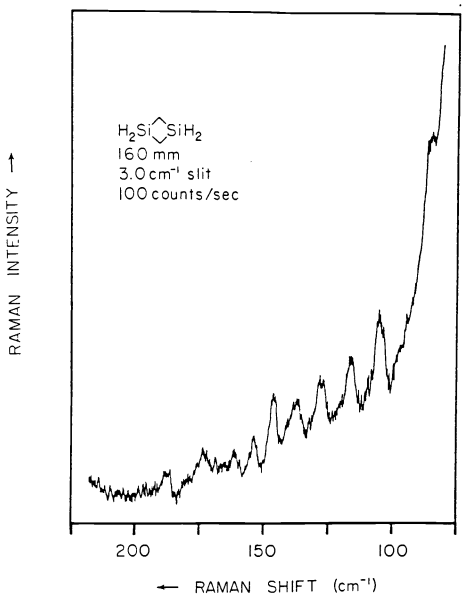

Fig. 8. Raman spectrum of 1,3-disilacyclobutane (ref. 8).

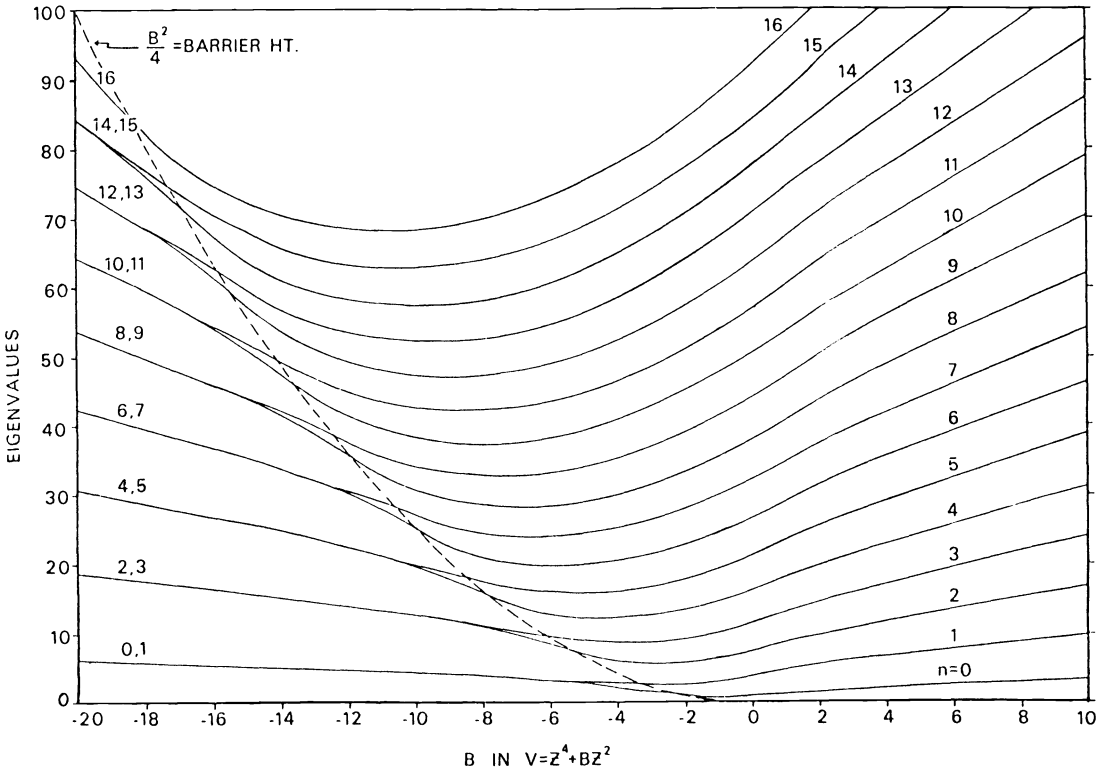

Fig. 9. Eigenvalues of the potential function $V = A(Z^4 - BZ^2)$ as a function of B (ref. 9).

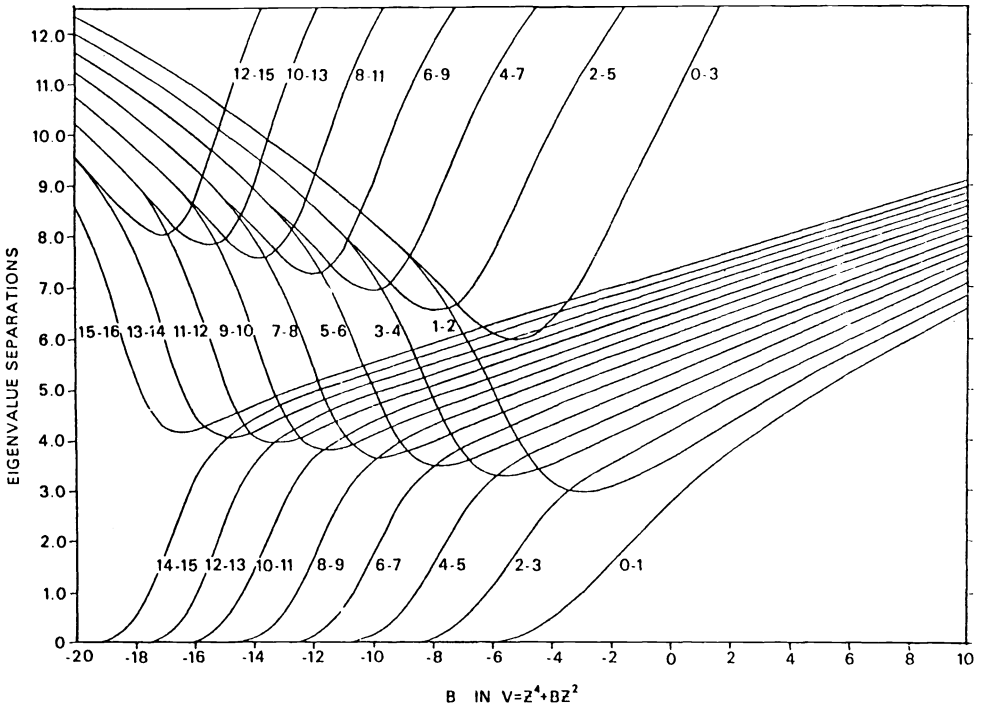

Fig. 10. Eigenvalue differences for $V = A(Z^4 - BZ^2)$ as a function of B (ref. 9).

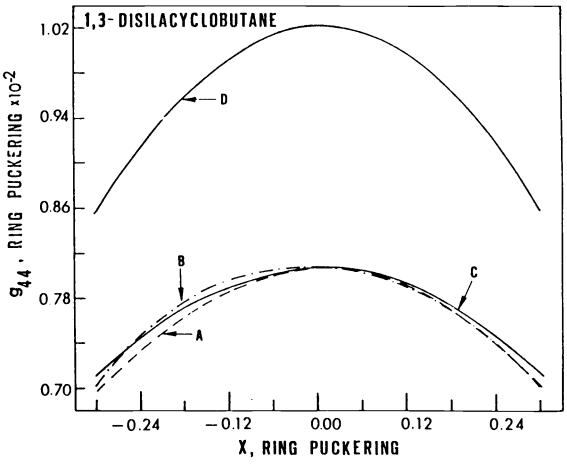

Fig. 11. Variation of reciprocal reduced mass (g_{44}) with puckering coordinate for 1,3-disilacyclobutane. Curves A-D represent different assumptions (ref. 11).

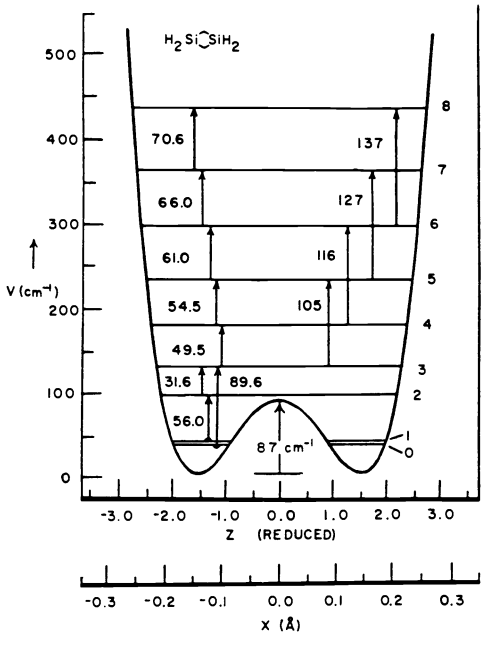

Fig. 12. Ring-puckering potential energy function for 1,3-disilacyclobutane (ref.8).

The approach described above has a deficiency in that the reduced mass in the wave equation is actually a function of coordinate [i.e., $\mu(x)$], and this variation is not accounted for in the published tables. Detailed procedures for calculating the kinetic energy (reciprocal reduced mass) expressions

$$g_{44}(x) = \sum_{i=0} g_{44}^{(i)} x^i \tag{7}$$

have been presented (refs. 10,11). Figure 11 shows the variation of $g_{44}(x)$ for DSCB as a function of puckering coordinate. The expansion in Eq. (7) is used as part of the Hamiltonian

$$H = \frac{\hbar^2}{2} \frac{d}{dx} g_{44}(x) \frac{d}{dx} + V \tag{8}$$

in order to properly calculate the energy levels. When this is done for DSCB, the potential function is determined to be

$$V = 2.3 \times 10^5 x^4 - 9.0 \times 10^3 x^2. \tag{9}$$

This is shown in Fig. 12. The barrier to planarity is 87 cm^{-1}, and the potential energy minimum corresponds to a dihedral angle of puckering of 24°.

The ring-puckering energy levels can also be determined from combination band spectra in the mid-infrared and Raman. For DSCB numerous series were observed (ref. 12); three overlapping series in the infrared SiH_2 stretching region are shown in Fig. 13, and one in the same region of the Raman spectrum is presented in Fig. 14.

When isotopic species of the same molecule are studied, it is expected that the potential functions for all such species should be the same. However, when the most simple "bisector model" of puckering was used to calculate the reduced masses for DSCB and its 1,1,3,3-d_4 derivative, different dimensioned potential functions were calculated for the two molecular species. This indicated that the vibrational model representing pure puckering is overly simple. In fact, when SiH_2 rocking (defined as β in Fig. 2) was allowed to mix in with the puckering motion to a modest degree, a single potential function was found which satisfactorily calculated the puckering levels for both molecules. This was presented as Eq. (9).

Further evidence that the puckering vibration is coupled to other motions came from the combination and hot band spectra involving the ring deformation and SiH_2 rocking modes. Figures 15 and 16 show the infrared and Raman spectra in the frequency region of these two vibrations. The data here, along with the observation of puckering spectra originating

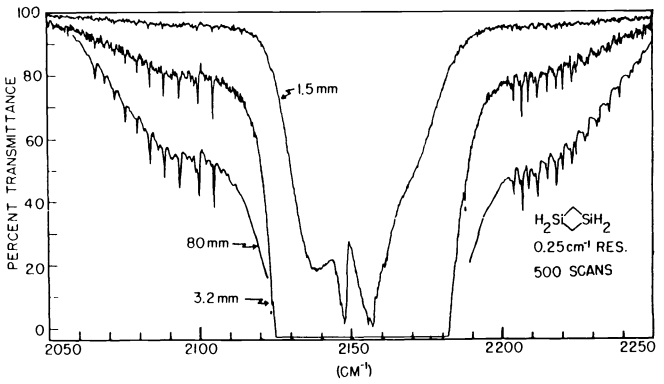

Fig. 13. Infrared combination bands of 1,3-disilacyclobutane in the SiH_2 stretching region (ref. 12).

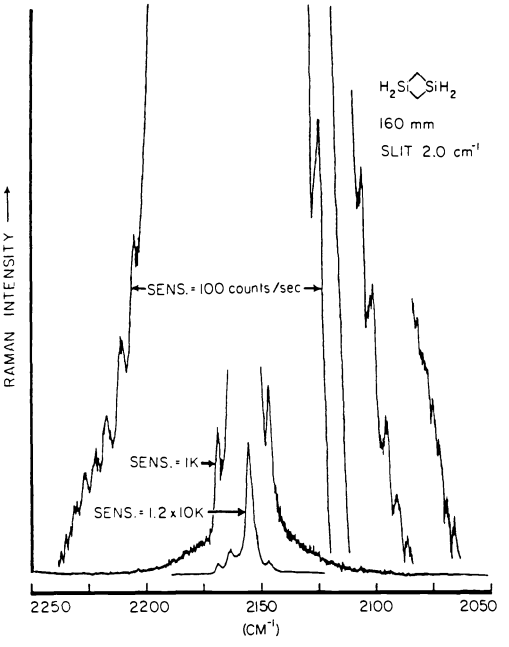

Fig. 14. Raman combination bands of 1,3-disilacyclobutane in the SiH_2 stretching region (ref. 12).

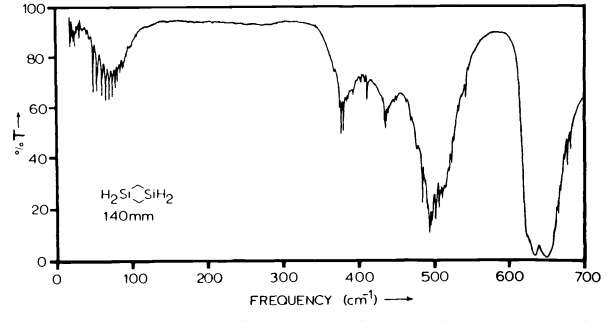

Fig. 15. Low-frequency infrared spectrum of 1,3-disilacyclobutane (ref. 13).

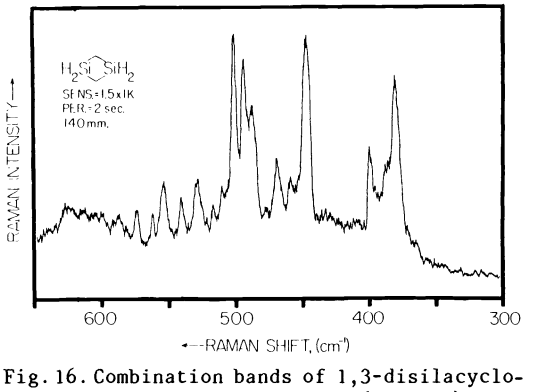

Fig. 16. Combination bands of 1,3-disilacyclobutane in the Raman spectrum (ref. 13).

from the excited state of the SiH_2 rocking, made it possible to determine the puckering levels in the excited states of the SiH_2 rocking and ring deformation modes. These are shown in Fig. 17. From these levels a three-dimensional potential energy surface for the puckering (x_1), deformation (x_2), and rocking (x_3) modes of DSCB was calculated. The form of the function is

$$V = ax_1^4 + bx_1^2 + cx_2^2 + dx_3^2 + ex_1^2x_2^2 + fx_1^2x_3^2. \tag{10}$$

The calculation of the energy levels for this potential energy function required symmetry factoring of the Hamiltonian matrix into eight blocks and the formation of the basis set from the product of one-dimensional solutions (ref. 3). The coefficients determined for the potential energy parameters are listed in Table II. Figures 18 and 19 show the two-dimensional slices of the three-dimensional surface when one of the vibrational coordinates is set equal to zero. The calculated surface very reliably reproduces all of the observed data, including that for the excited states. It also demonstrates that the puckering and ring-deformation are cooperative vibrations and the puckering and in-phase SiH_2 rocking are anti-cooperative. The barrier to planarity calculated three-dimensionally is 87 cm^{-1}, the same as for the one-dimensional calculation.

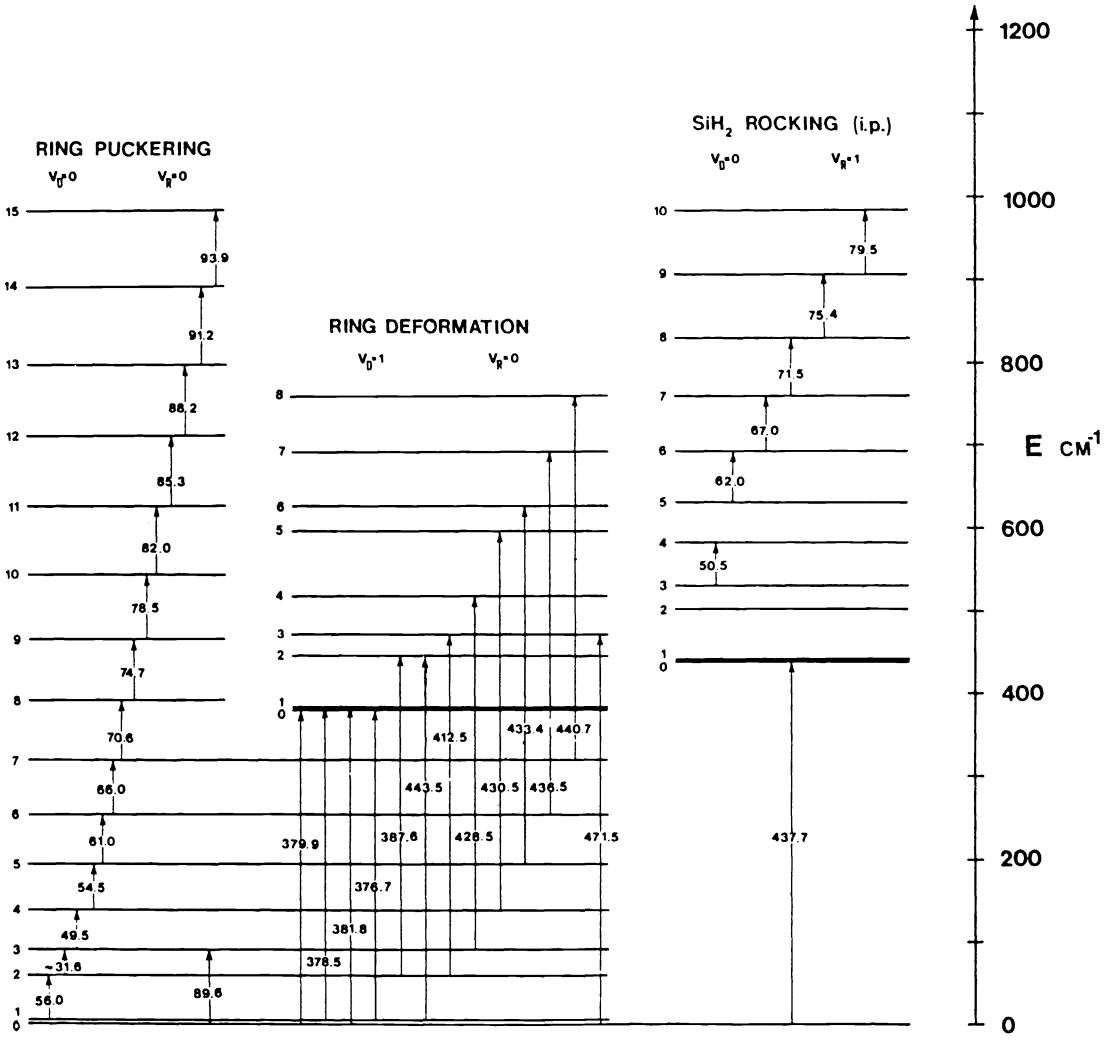

Fig. 17. Ring-puckering levels of 1,3-disilacyclobutane in the ground and excited states of the in-phase SiH_2 rocking and angle deformation modes (ref. 13).

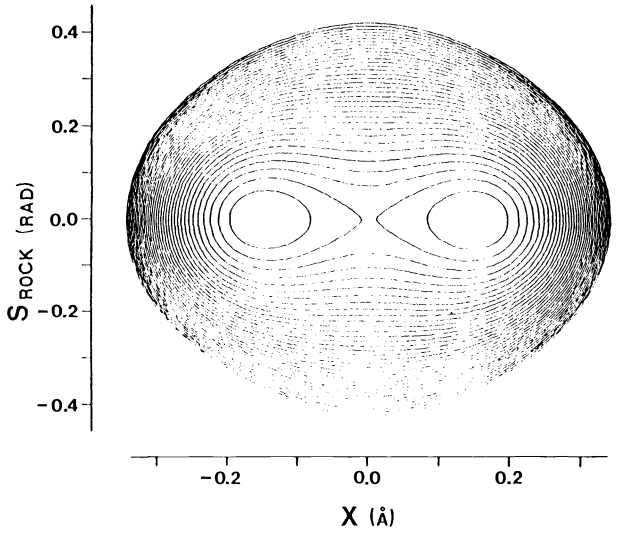

Fig. 18. Two-dimensional slice of 1,3-disilacyclobutane potential surface with S_{DEF} = 0 (ref. 13).

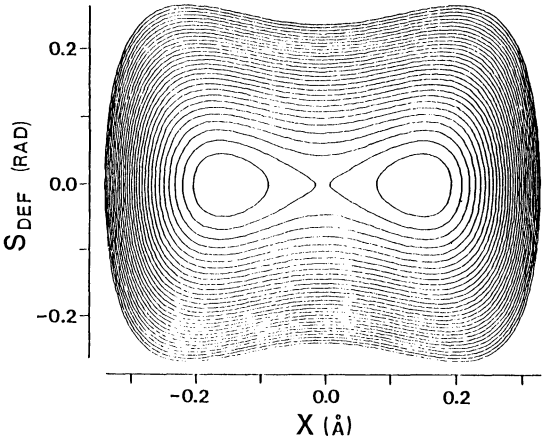

Fig. 19. Two-dimensional slice of 1,3-disilacyclobutane potential surface with S_{ROCK} = 0 (ref. 13).

While the study described above represents the only three-dimensional analysis for a ring molecule, one-dimensional potential energy functions have been determined for several other four-membered rings. The barriers to inversion for these are shown in Table III. The barriers, if any, in general arise from torsional forces between methylene (or similar) groups since these tend to favor non-planar conformations for which the CH_2 groups are not eclipsed. Angle strain forces tend to favor planar structures for which the ring angles are at maximum values. The molecular mechanics (MM2) methods of Allinger (ref. 14), which utilize these forces to predict the minimum energy structures, were used to estimate the barriers to inversion for a few of those molecules (ref. 15). These are also shown in Table IV. While the MM2 values are far from perfect, it can be seen that they are the right order of magnitude.

TABLE II. Three-dimensional potential energy and kinetic energy functions for the vibrations of 1,3-disilacyclobutane

Potential Parameters

$$V = a_1x_1^4 + b_1x_1^2 + b_2x_2^2 + b_3x_3^2 + c_{12}x_1^2x_2^2 + c_{13}x_1^2x_3^2$$

$a_1 = 1.966 \times 10^5$ cm^{-1}A^{-4} $\quad b_1 = -7.969 \times 10^3$ cm^{-1}A^{-2}

$b_2 = 2.230 \times 10^4$ cm^{-1}rad^{-2} $\quad b_3 = 6.823 \times 10^3$ cm^{-1}rad^{-2}

$c_{12} = -1.096 \times 10^5$ cm^{-1}A^{-2}rad^{-2} $\quad c_{13} = 1.359 \times 10^5$ cm^{-1}A^{-2}rad^{-2}

Kinetic Energy Functions

$g_1 = 8.074 \times 10^{-3} - 1.132 \times 10^{-2}x_1^2 - 4.921 \times 10^{-2}x_1^4 + 2.019 \times 10^{-2}x_1^6$ $\quad \mu_1 = 123.86$ amu

$g_2 = 0.106$ amu^{-1} $\quad \mu_2 = 9.45$ amu

$g_3 = 0.403$ amu^{-1} $\quad \mu_3 = 2.48$ amu

Harmonic Frequencies

$\bar{\nu}_1 = 40.0$ cm^{-1} $\quad \bar{\nu}_2 = 398.6$ cm^{-1} $\quad \bar{\nu}_3 = 430.8$ cm^{-1}

x_1 = ring-puckering (A) $\quad x_2$ = ring-puckering (rad) $\quad x_3$ = SiH_2 (i.p.) rock (rad)

TABLE III. Experimental and calculated barriers to inversion of four-membered ring molecules

Molecule	Barrier (cm^{-1}) Expt.[a]	Barrier (cm^{-1}) Calc.[b]	Dihedral Angle Expt.[a]	Dihedral Angle Calc.[b]
$CH_2CH_2CH_2CH_2$	515	321	29	28
$CH_2CH_2CH_2SiH_2$	440	433	35	32
$CH_2SiH_2CH_2SiH_2$	87		24	
$CH_2CH_2CH_2O$	15	0	0	0
$CH_2CH_2CH_2S$	274	150	28	27
$CH_2CH_2CH_2Se$	375			
$CH_2CH_2CH_2NH$	441[c]			
$CH_2CH_2CH_2C{=}O$	8	0	0	0
$CH_2OCH_2C{=}O$	0		0	
$CH_2OCH_2C{=}O$	0		0	
$CH_2CH_2CH_2C{=}CH_2$	140			
$CH_2OCH_2C{=}CH_2$	0		0	
$CH_2C(O)OC{=}CH_2$	0		0	

[a]From Ref. 59 and references therein.
[b]From molecular mechanics (MM2) calculations (Ref. 15).
[c]Asymmetric potential with 91 cm^{-1} energy difference between minima.

TABLE IV. Experimental and calculated barriers to inversion of cyclopentene analogs

Molecule	Barrier (cm^{-1}) Experimental[a]	Barrier (cm^{-1}) Calculated[b]
$CH_2CH{=}CHCH_2CH_2$	232	253
$CH_2CH{=}CHCH_2O$	0	0
$CH_2CH{=}CHCH_2S$	0	0
$CH_2CH{=}CHCH_2C{=}O$	0	
$CH_2H{=}CHCH_2SiH_2$	0	
$CH_2CH{=}CHCH_2NH$	55[c]	
$CH_2CH{=}CHCH_2PH$	331[d]	
$CH_2N{=}NCH_2CH_2$	113	
$CH_2CH{=}CHOCH_2$	83	0
$CH_2CH{=}CHSCH_2$	325	169
$CH_2CH{=}CHSiH_2CH_2$	0	114
$CH_2CH{=}CHC(O)CH_2$	0	0
$CH_2CH{=}CHPHCH_2$	205[e]	

[a]From Ref. 59 and references therein.
[b]MM2 calculations (ref. 15 and 60).
[c]Asymmetric function with 45 cm^{-1} difference between energy minima.
[d]Asymmetric function with single minimum (ref. 25); the exo conformer is 785 cm^{-1} less stable then the endo conformer.
[e]Asymmetric function with single minimum (ref. 63); the exo conformer is 524 cm^{-1} less stable than the endo conformer.

FIVE-MEMBERED RINGS

Pseudo-four-membered rings

Cyclopentene and analogous molecules have been classified as pseudo-four-membered rings since their puckering motions resemble those of four-membered-rings (the atoms joined by the double bond behave as a single atom during the puckering). The first far-infrared spectra for such molecules were reported in 1967 for cyclopentene by Laane and Lord (ref. 16) and for 2,5-dihydrofuran by Ueda and Shimanouchi (ref. 17). The first Raman spectra (refs. 18,19) for these molecules were reported in 1972. Table IV presents the barriers determined for the pseudo-four-membered ring molecules along with calculated MM2 values for several of these (ref. 15). As an example of the experimental data, Fig. 20 shows the far-infrared and Raman spectra recorded for cyclopentene-1-d_1, along with the one-dimensional potential energy function (ref. 20).

The far-infrared spectra of these types of molecules often show a "side-band series" in addition to the main series of bands. Laane and Lord (ref. 16) recognized that these bands originate when the molecule is in the excited state of the ring-twisting. The frequency shifts between the two series reflect the interaction between the two motions. Carreira,

Mills, and Person (ref. 21) carried out the first two-dimensional study of these two motions for the planar 2,5-dihydrofuran molecule. More recently, Laane and co-workers have completed two-dimensional analyses for cyclopentene (ref. 22) (4 isotopic species) and silacyclopent-3-ene (ref. 23) (3 isotopic species). Figure 21 shows the energy levels for the d_1 and d_4 isotopic species of cyclopentene; these were used to help determine the potential energy surface shown in Fig. 22. The barrier to planarity is 232 cm^{-1}. Figure 23 shows the surface for the planar silacyclopent-3-ene.

A particularly interesting two-dimensional study was completed recently on the ring-puckering and P-H inversion motions of 3-phospholene (ref. 24). Figure 24 shows how each of these motions can convert from one-puckered conformation to the other. Figure 25 shows

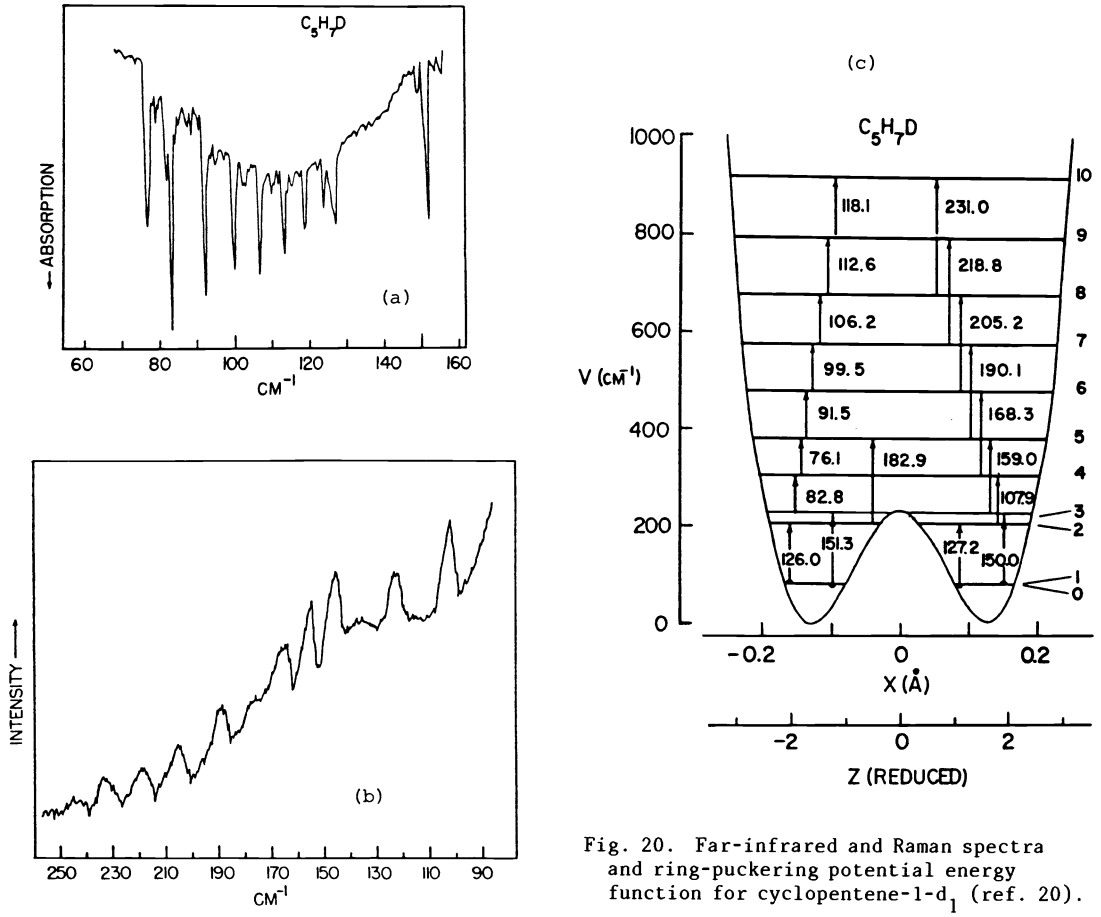

Fig. 20. Far-infrared and Raman spectra and ring-puckering potential energy function for cyclopentene-1-d_1 (ref. 20).

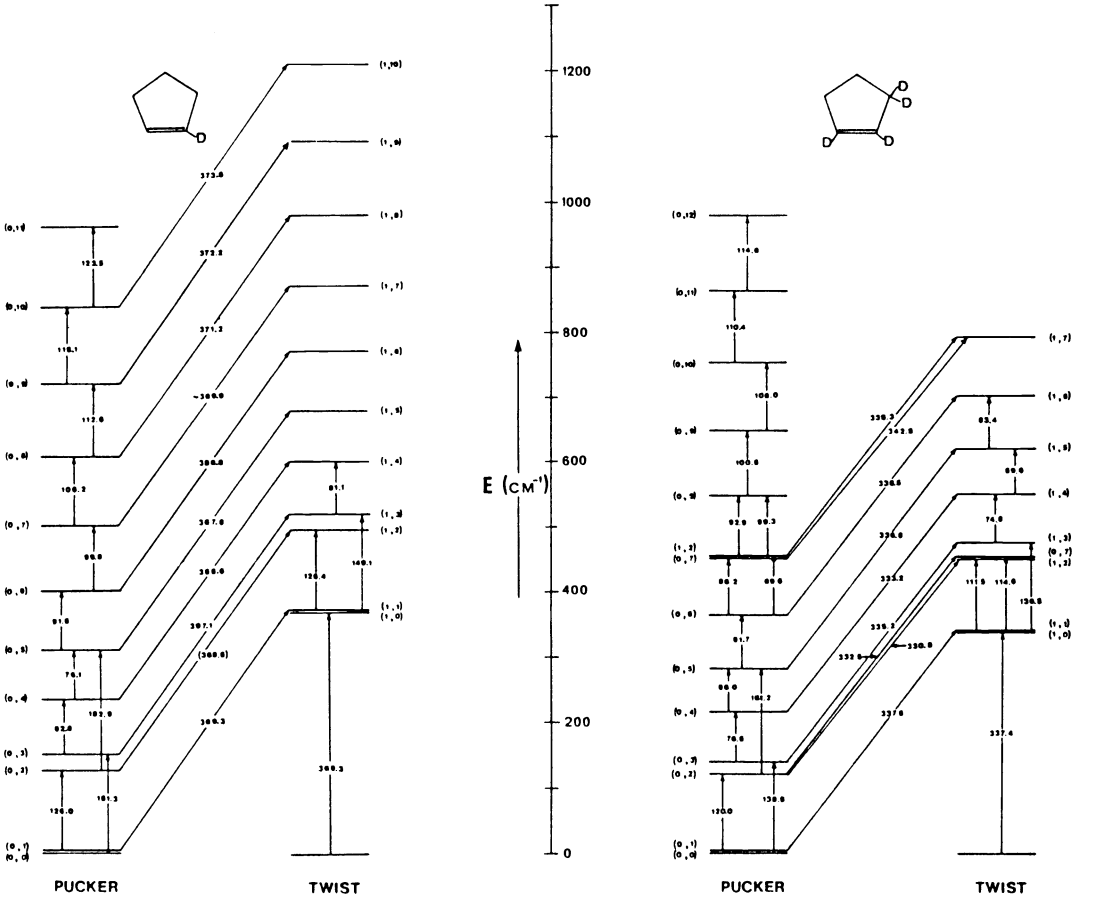

Fig. 21. Energy levels for the puckering and twisting levels of cyclopentene-1-d_1 and -1,2,3,3-d_4 (ref. 20).

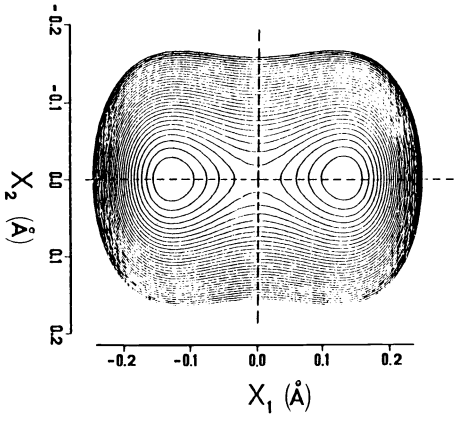

Fig. 22. Potential energy surface for the puckering and twisting of cyclopentene (ref. 22).

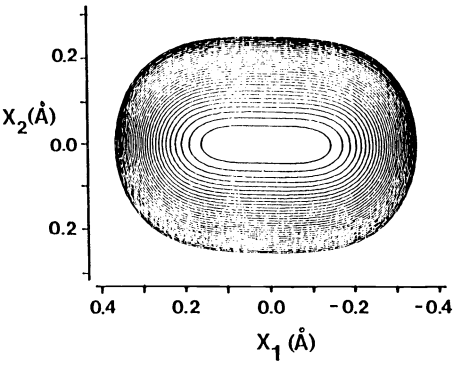

Fig. 23. Potential energy surface for the puckering (x_1) and twisting (x_2) of silacyclopent-3-ene (ref. 23).

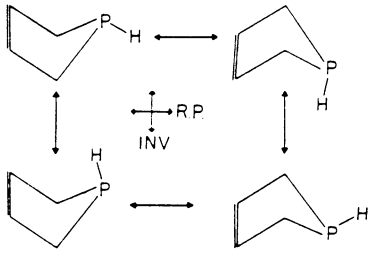

Fig. 24. Conformational changes of 3-phospholene (ref. 25).

the far-infrared spectrum of this molecule and Fig. 26 presents the energy levels and the infrared and Raman transitions associated with both the puckering and inversion vibrations (ref. 25). The analysis of the data required the use of Van Vleck perturbation methods along with other special computational techniques (ref. 26). The potential surface determined is shown in Fig. 27; this reproduces very well all of the experimental data for the ground and excited state of two isotopic species. The surface demonstrates that only the endo conformer has a potential minimum, with a puckering angle of 18°; the exo conformer lies 785 cm^{-1} higher in energy. The PH inversion encounters a high barrier of about 5500 cm^{-1}. The proper representation of the quite substantial coupling between the two motions is critical for correctly calculating the transition frequencies.

Pseudorotators

Following the prediction of free pseudorotation for cyclopentane (ref. 5), Durig and Wertz (ref. 27) first observed the combination band spectra for this molecule in 1968. A higher resolution spectrum recorded more recently (ref. 28) is shown in Fig. 28. The data confirm that the pseudorotation is indeed very nearly free, that is, with essentially no energy differences existing between the bent and twisted forms of cyclopentane. Carreira et al. (ref. 45) have combined the infrared combination data with the Raman data of the radial motion to calculate a two-dimensional surface in terms of the bending and twisting motions of cyclopentane. Bauman and Laane (ref. 28) have extended the study to include six isotopic forms of cyclopentane and have found essentially the same barrier to planarity (1808 cm^{-1}) and no measurable barrier to pseudorotation.

Cyclopentane-like rings containing heteroatoms are expected to have barriers to pseudorotation. For both tetrahydrofuran and 1,3-dioxolane (ref. 38) these barriers are less than 100 cm^{-1} and the pseudorotation is nearly unhindered. However, for silacyclopentane there is a large energy difference between its bent and the more stable twist forms. Based on the far-infrared spectrum of this molecule, Laane (ref. 48) used a periodic pseudorotational potential function to calculate a barrier of pseudorotation of about 1400 cm^{-1}. The data of Durig and Willis (ref. 49) on the deuterated species were compatible with this interpretation. The Raman spectra of the radial mode (Fig. 29) recorded later made it possible to carry out a two-dimensional surface calculation (ref. 50), and a barrier to planarity of 1454 cm^{-1} was estimated. However, Wells and Laane (ref. 51) have recently reexamined the data for silacyclopentane $-d_0$ and $-d_2$ along with new data for the d_1 species (shown in Fig. 30) and have found that the simple two-dimensional harmonic oscillator basis set used for the calculations was not adequate for correctly calculating the energy levels. In fact, the data, when analyzed with improved basis sets, predict a barrier approximately twice as high. Molecular mechanics calculations estimate a barrier (ref. 52) of 2062 cm^{-1} and this value should be in the correct range. What is evident here is that there is some difficulty in correctly extrapolating to a high barrier height when the experimental data do not go to high enough energies. This type of problem will be examined in more detail under the discussion of cyclohexene-like molecules.

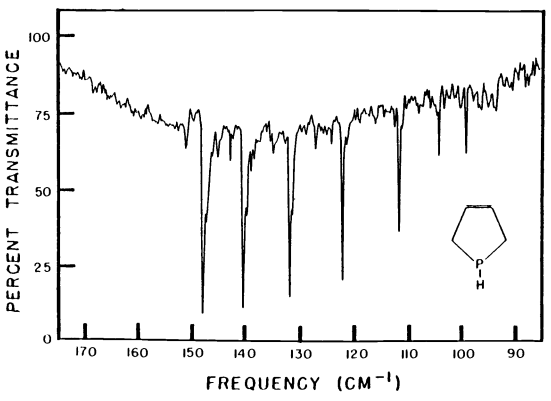

Fig. 25. Far-infrared spectrum of 3-phospholene (ref. 25).

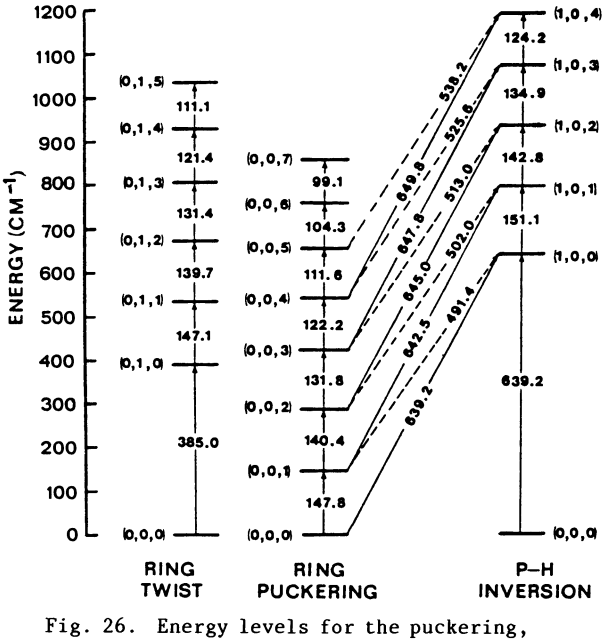

Fig. 26. Energy levels for the puckering, PH inversion, and ring twisting of 3-phospholene (ref. 25).

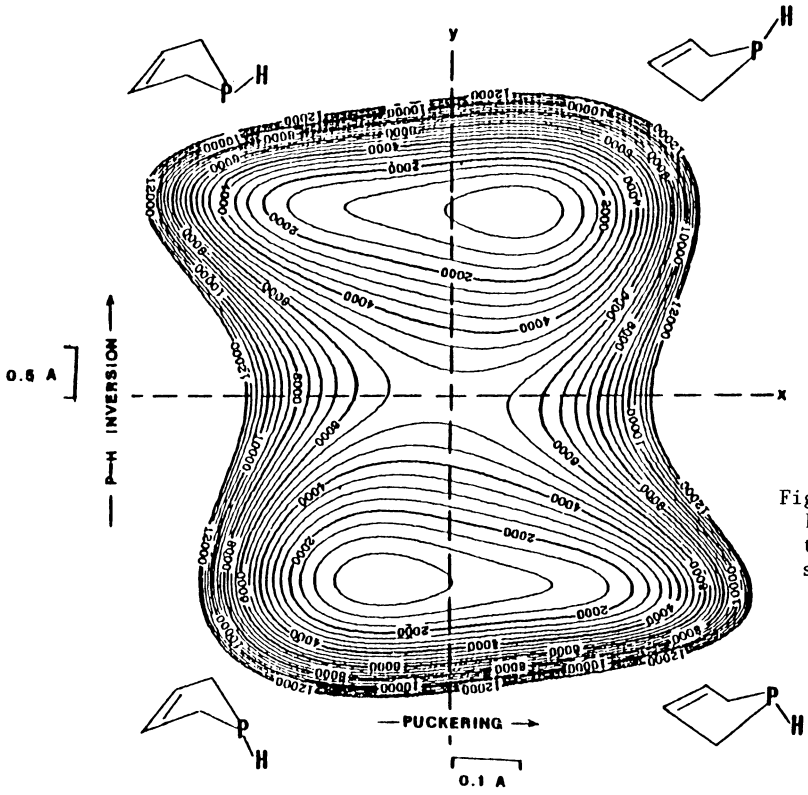

Fig. 27.
Potential energy surface for the puckering and PH inversion of 3-phospholene (ref. 26).

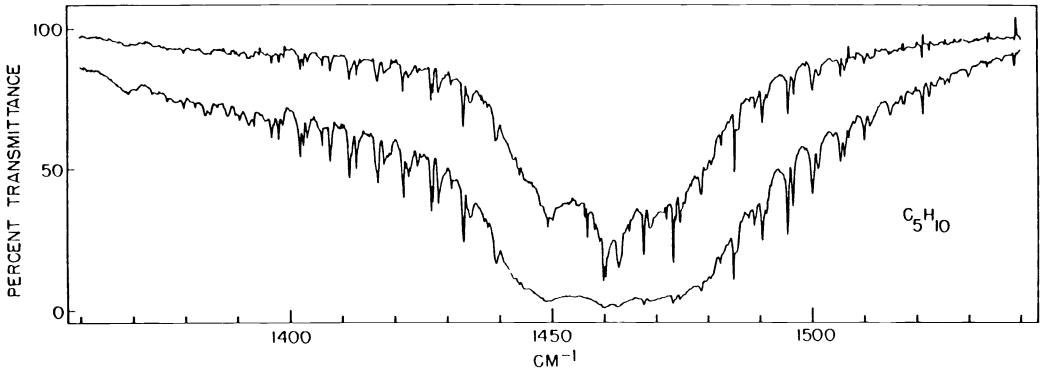

Fig. 28. Pseudorotational combination bands of cyclopentane (ref. 28).

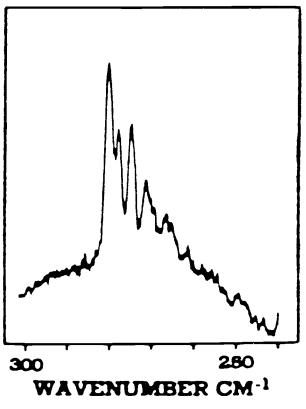

Fig. 29. Raman spectrum of the radial mode of silacyclopentane (ref. 50).

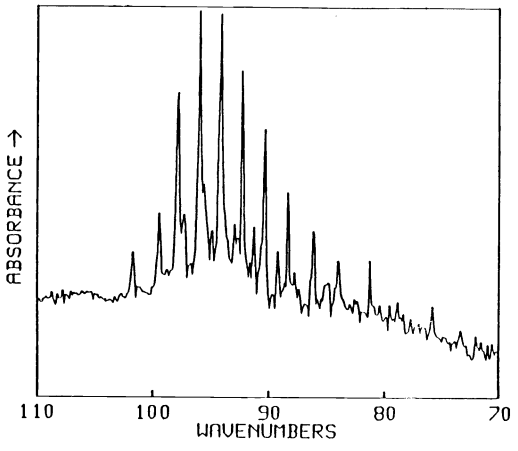

Fig. 30. Pseudorotational spectrum of silacyclopentane-1-d (ref. 51).

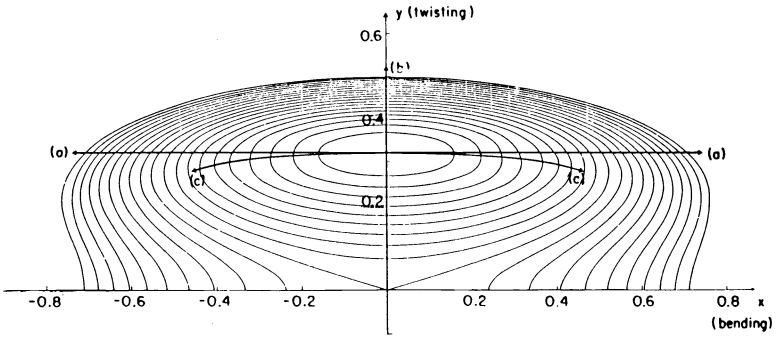

Fig. 31. Potential energy of cyclopentanone in terms of bending and twisting coordinates (ref. 46).

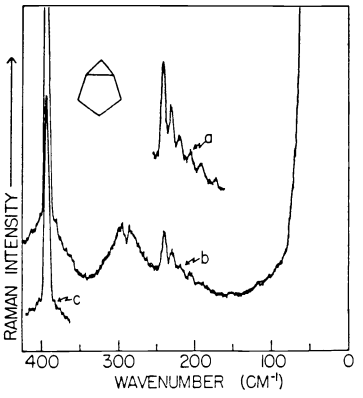

Fig. 32. Raman spectrum of bicyclo[3.1.0]hexane (ref. 43).

The cyclopentanone molecule, which might be expected to be a pseudorotator, has been studied by Ikeda and Lord (ref. 46) and been shown to have a stable twisted (C_2) conformation. However, it interconverts, as shown in Fig. 31, from one twist form to the other via the planar structure. The two-dimensional surface was determined from the far-infrared spectra of four different isotopic species.

Bicyclic molecules with five-membered rings

The far-infrared and Raman spectra of several bicyclohexane and bicycloheptene type molecules including

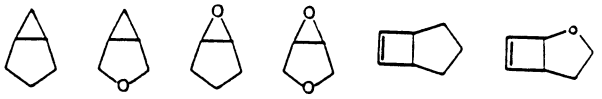

have been examined (refs. 40,42,43,53). Each of these can be considered to be a pseudo-four-membered ring since the smaller ring rigidly fixes two of the atoms in the five-membered ring to lie in the plane of the smaller ring. The Raman spectrum of bicyclo[3.1.0]hexane (ref. 43) (A) is shown in Fig. 32 and the ring-puckering potential energy function determined from this data is presented in Fig. 33. The results demonstrate that the molecule has a single minimum (corresponding to the boat conformer) in the potential function, and the second puckered (chair) and planar conformations lie 1000 to 2000 cm^{-1} higher in energy. The asymmetric potential functions for the other molecules above are similar in having single minima corresponding to boat conformations.

The low-frequency vibrations of 2-oxabicyclo[3.2.0]hept-6-ene (F) are interesting due to their extensive interaction with one another (ref. 53). Figure 34 shows the infrared ring-twisting spectrum and Fig. 35 shows the energy map for the molecule based on both infrared and Raman data for the four low-frequency modes.

SIX-MEMBERED RINGS

Cyclohexadienes and analogs

Laane and Lord (ref. 41) have examined the far-infrared spectrum of 1,4-cyclohexadiene (a pseudo-four-membered ring) and observed seven closely spaced bands near 108 cm^{-1}. The results showed the molecule to have a planar ring rather than the boat form indicated by an earlier electron diffraction study (ref. 54). MM2 calculations (ref. 52) and Raman spectra (ref. 55) later confirmed the planar structure.

The far-infrared data for 1,4-dioxadiene are more anharmonic but also show that this molecule is planar (ref. 57). On the other hand, 1,3-cyclohexadiene has been determined to be twisted with a barrier of about 1100 cm^{-1} based on the analysis of the Raman spectrum of the ring-twisting motion (ref. 55).

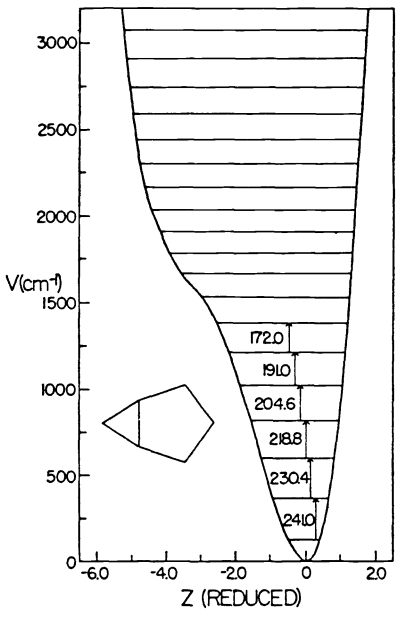

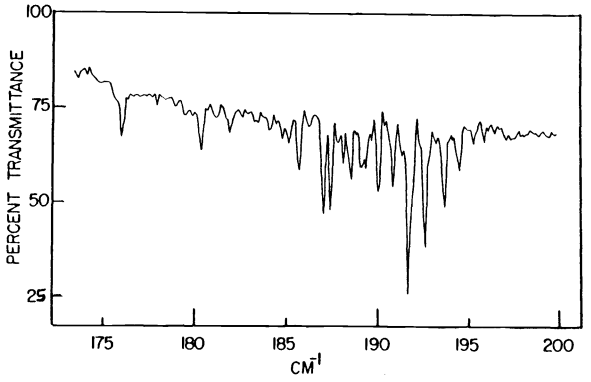

Fig. 34. Infrared spectrum of the ring-twisting mode of 2-oxabicyclo[3.2.0]hept-6-ene (ref. 43).

← Fig. 33. Ring-puckering potential energy function of bicyclo[3.1.0]hexane (ref. 43).

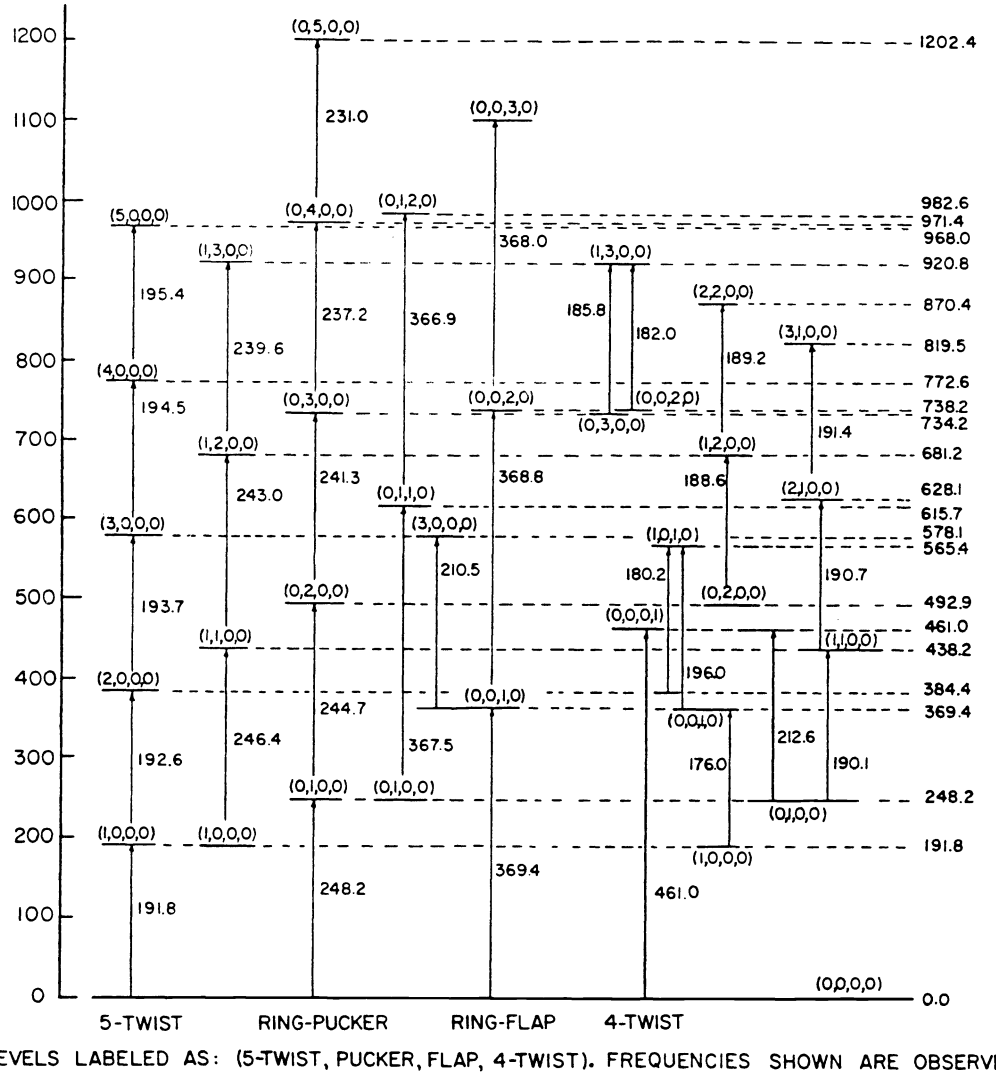

LEVELS LABELED AS: (5-TWIST, PUCKER, FLAP, 4-TWIST). FREQUENCIES SHOWN ARE OBSERVED

Fig. 35. Energy map for the four low-frequency vibrations of 2-oxabicyclo[3.2.0]hept-6-ene (ref. 53).

Cyclohexene and analogs

The study of cyclohexene and analogous molecules containing heteroatoms is currently an active area of investigation in our laboratory. Lord and co-workers (ref. 57) initially studied the far-infrared spectra of 1,4-dioxene and 2,3-dihydropyran and Durig et al. (ref. 58) recorded the corresponding Raman data. Figure 36 shows the far-infrared data near 190 cm^{-1} from the ring bending region and the difference bands near 100 cm^{-1} for 1,4-dioxene. The Raman spectrum of the ring-twisting is shown in Fig. 37, and Fig. 38 presents the pattern of observed transitions. A two dimensional surface with a barrier to planarity of over 7000 cm^{-1} and a barrier to interconversion (from the more stable twisted form to the bent form) of about 3200 cm^{-1} were calculated. The energy difference between the twisted and bent forms was estimated to be about 1600 cm^{-1}. It was noted (ref. 59), however, that since the experimental data only extend up to about 1500 cm^{-1}, extrapolations beyond that point are rather speculative. Figure 39 shows cross sections of the published potential surface. That on the left is along the twisting axis, and the estimate for the barrier to planarity can be seen to require substantial extrapolation. The curve on the right represents the interconversion path between twist and bent forms. Here again the data is less than desired for establishing the nature of the surface. The dotted portion of the curve indicates that the presence of a minimum for the bent form is not clear cut (ref. 59). A similar potential energy surface (with similar questions regarding extrapolation) has been derived for 2,3-dihydrpyran (ref. 57).

In our laboratory we have been studying the infrared and Raman spectra of cyclohexene and have worked to obtain a consistent potential surface model to explain the data for this molecule along with that for the two oxygen analogs. To aid our interpretation we have used molecular mechanics methods to estimate the energy differences between the various conformers. Our MM2 calculations on four- and five-membered ring molecules have convinced us that values calculated for barrier heights will generally not be more than several hundred cm^{-1} in disagreement with experimental results. Table V shows the results from molecular mechanics calculations for the barriers to planarity and the energy differences between twisted and bent forms for several cyclohexene-like molecules (ref. 60). The results for the oxygen molecules discussed above strongly suggest that the previous interpretation of the data is erroneous. We have determined potential energy surfaces for 1,4-dioxene (ref. 60), 2,3-dihydropyran (ref. 60), and cyclohexene (ref. 61) which not only fit the experimental data better, but also are much more compatible with the MM2 results. Figure 40 shows the surface which we have determined for 2,3-dihydropyran. This has a barrier to planarity of 3676 cm^{-1} and an energy difference of 3194 cm^{-1} between bent and twisted forms. These values compare favorably with those in Table V.

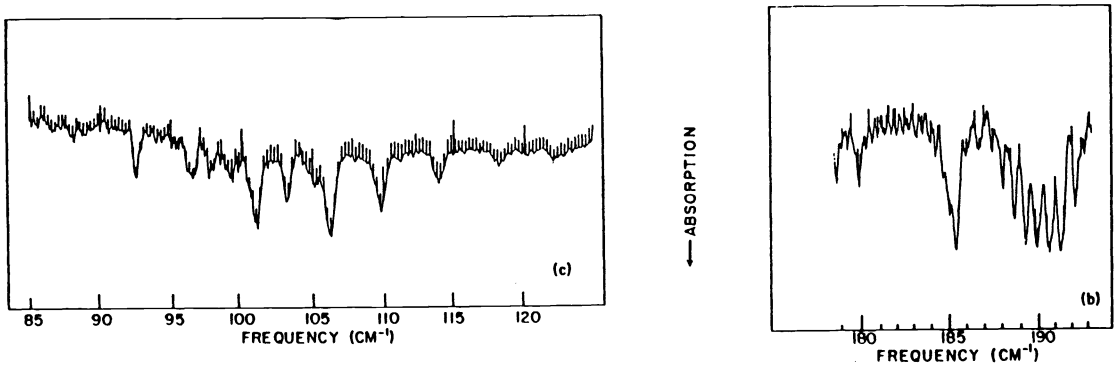

Fig. 36. Far-infrared spectra of 1,4-dioxene in the ring-bending and difference band regions (ref. 57).

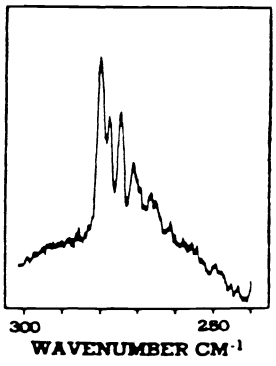

Fig. 37. Raman spectrum of the ring-twisting of 1,4-dioxene (ref. 58).

TABLE V. Calculated[a] conformational energy differences of cyclohexene and analogs

Molecule	Energy difference (cm^{-1}) Barrier to planarity	$\Delta E(b,t)$[b]
$\overline{CH=CHCH_2CH_2CH_2CH_2}$	3790	2119
$\overline{CH=CHCH_2CH_2CH_2O}$	3078	2956
$\overline{CH=CHOCH_2CH_2O}$	2294	2294
$\overline{CH=CHCH_2CH_2CH_2SiH_2}$	3602	2147

[a]From MM2 molecular mechanics calculations (ref. 60).
[b]Energy difference between bent and twisted forms.

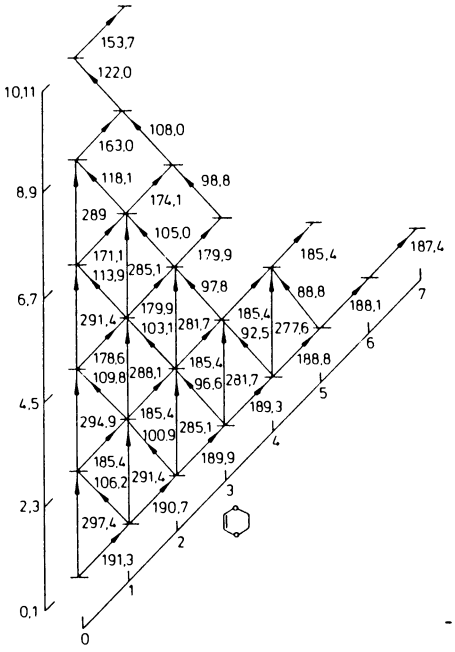

Fig. 38. Energy level pattern for the twisting and bending of 1,4-dioxene (ref. 59).

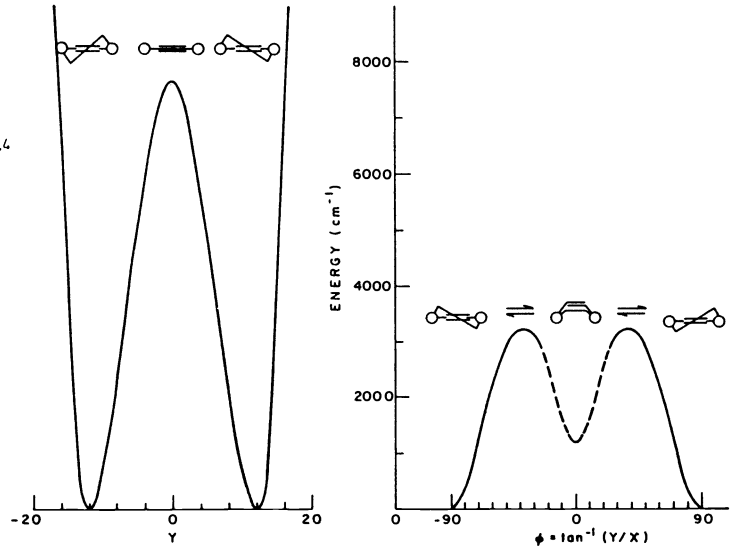

Fig. 39. Cross sections of published 1,4-dioxene potential surface (ref. 59).

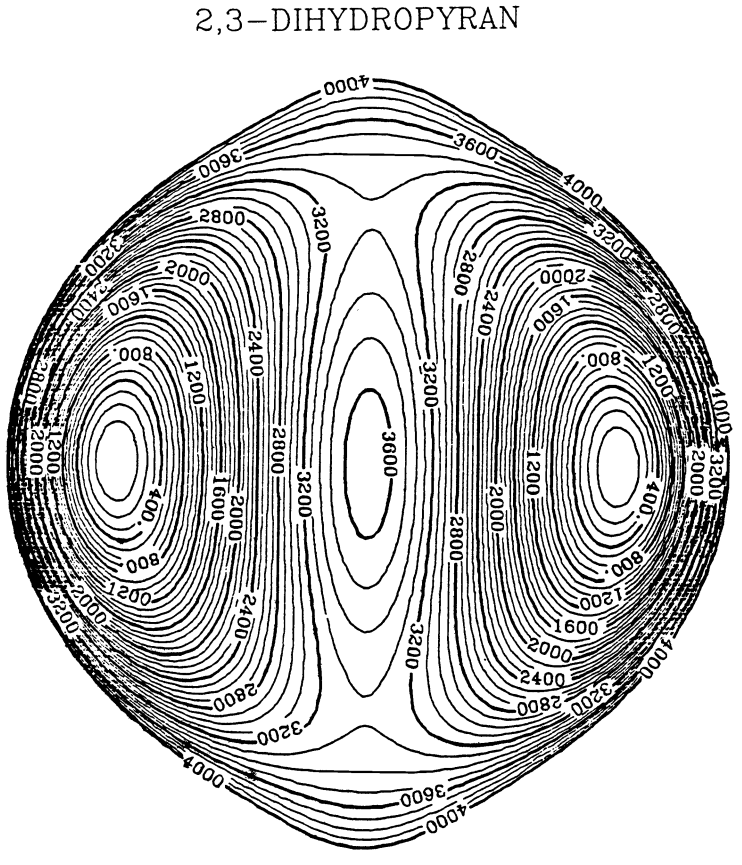

Fig. 40. Potential energy surface for 2,3-dihydropyran (ref. 60).

Cyclohexane

The conformations of cyclohexane, with its more stable chair form, have been extensively studied by nmr and other methods, and its interconversion processes are reasonably well understood. Nonetheless, an accurate vibrational potential energy surface has not been determined. Because the energy barriers between the chair, boat, and planar conformations are substantial, extrapolation of data at lower energies to determine the barriers presents difficulties similar to those discussed for cyclohexene (see Fig. 39). Moreover, spectroscopic data for the three low-frequency ring modes effecting conformational changes have been sparse.

Figure 41 presents the low-frequency Raman spectrum of the ring-bending motion (which would take the chair form through the planar structure to the flipped chair conformer) of cyclohexane, which we have recorded in our laboratory (ref. 62). Additional data on the other ring motions is required to reliably determine the three-dimensional surface appropriate for characterizing the conformational changes for the molecule. With the limited data avilable, it is possible only to estimate a one-dimensional ring-bending potential function. Use of the reduced potential in Eq. 6 produces the parameters A = 22.3 cm^{-1} and B = -37.5, and this function fits the data very well. The barrier to inversion calculated from this function is about 7800 cm^{-1}, and this is about twice the known value.

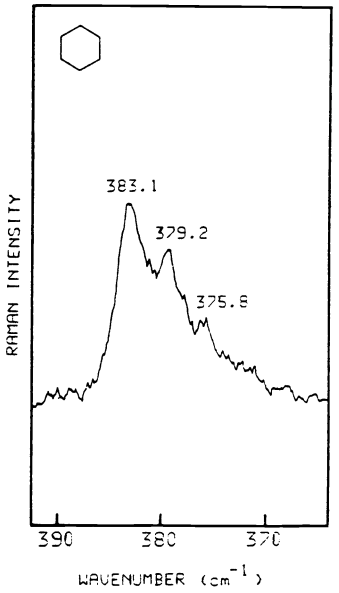

Fig. 41. Raman spectrum of cyclohexane (ref. 62).

The problem clearly lies in the overly simple form of the potential function used, and in the lack of data at higher energies. The conclusion to be drawn is that considerable care must be used in assessing calculations which determine a barrier substantially higher than the available data.

CONCLUSION

Several earlier reviews (ref. 59,64-69) on vibrational potential energy functions have been published. The present paper has not tried to be comprehensive, but rather attempted to highlight the current emphasis on the use of two- or three-dimensional potential energy surfaces and the improved methods of calculation. The analysis of potential functions for internal rotations, a major research area (see, for example, refs. 70-73), has not been considered here.

Current studies tend to focus on larger ring systems (such as the cyclohexene analysis) which often have complicated potential surfaces and sizable barriers. For such molecules it is often necessary to record spectra for several isotopic species and to use complementary information (such as results of molecular mechanics calculations) to determine meaningful potential functions.

An exciting prospect for the future is the determination of vibrational potential energy surfaces in electronic excited states. We are currently initiating fluorescence, electronic absorption, and resonance Raman investigations in order to achieve this.

Acknowledgements

Much of the work described here was carried out by the former students and associates cited in the references, and they deserve full credit for their achievements. The National Science Foundation and Robert A. Welch Foundation have provided the funds without which no results could have been achieved.

REFERENCES

1. J. Laane and R. C. Lord, J. Chem. Phys., 48, 1508 (1968).
2. J. D. Lewis, T. H. Chao, J. Laane, J. Chem. Phys., 62, 1932 (1975).
3. W. E. Milne, Phys. Rev., 35, 863 (1930).
4. R. P. Bell, Proc. Roy. Soc. (London), A183, 328 (1945).
5. J. E. Kilpatrick, K. S. Pitzer, and R. Spitzer, J. Amer. Chem. Soc., 75, 5634 (1947); K. S. Pitzer and W. Donath, J. Amer. Chem. Soc., 81, 3213 (1959).
6. R. J. Capwell and F. A. Miller, Spectrochem. Acta, 27A, 947 (1971).
7. J. M. R. Stone and I. M. Mills, Mol. Phys., 18, 631 (1970).
8. R. M. Irwin, J. M. Cooke, and J. Laane, J. Amer. Chem. Soc., 99, 3273 (1977).
9. J. Laane, Appl. Spectrosc., 24, 73 (1970).
10. J. Laane, M. A. Harthcock, P. M. Killough, L. E. Bauman and J. M. Cooke, J. Mol. Spectrosc., 91, 286 (1982).
11. M. A. Harthcock and J. Laane, J. Mol. Spectrosc., 91, 00 (1982).
12. R. M. Irwin and J. Laane, J. Mol. Spectrosc., 91, 300 982).
13. P. M. Killough, R. M. Irwin, and J. Laane, J. Chem. Phys., 76, 3890 (1982).
14. U. Burkett and N. L. Allinger, Molecular Mechanics, American Chemical Society Monograph 177, Washington, D.C., (1982).
15. R. Lee and J. Laane, unpublished results.
16. J. Laane and R. C. Lord, J. Chem. Phys., 47, 4941 (1967).
17. T. Ueda and T. Shimanouchi, J. Chem. Phys., 47, 4042 (1967).
18. T. H. Chao and J. Laane, Chem. Phys. Lett., 14, 595 (1972).
19. J. R. Durig, A. C. Shing, L. A. Carreira, and Y. S. Li, J. Chem. Phys., 57, 4398 (1972).
20. J. R. Villarreal, L. E. Bauman, and J. Laane, J. Phys. Chem., 80, 1172 (1976).
21. L. A. Carreira, I. M. Mills, W. B. Person, J. Chem. Phys., 56, 4450 (1972).
22. L. E. Bauman, P. M. Killough, J. M. Cooke, J. R. Villarreal, and J. Laane, J. Phys. Chem., 86, 2000 (1982).
23. P. M. Killough and J. Laane, J. Chem. Phys., 80, 5475 (1980).
24. M. A. Harthcock and J. Laane, J. Chem. Phys., 79, 2103 (1983).
25. L. W. Richardson, P. W. Jagodzinski, M. A. Harthcock, and J. Laane, J. Chem. Phys., 73, 5556 (1980).
26. M. A. Harthcock and J. Laane, J. Phys. Chem., 89, 4231 (1985).
27. J. R. Durig and D. W. Wertz, J. Chem. Phys., 49, 2118 (1968).
28. L. E. Bauman and J. Laane, to be published.
29. A. Danti, W. J. Lafferty, and R. C. Lord, J. Chem. Phys., 33, 297 (1960).
30. S. I. Chan, J. Zinn, J. Fernandez, W. D. Gwinn, J. Chem. Phys., 33, 1643 (1960); S. I. Chan, J. Zinn, W. D. Gwinn, J. Chem. Phys., 34, 1319 (1961).
31. W. J. Lafferty, D. W. Robinson, R. V. St. Louis, J. L. Russell, and H. L. Strauss, J. Chem. Phys., 42, 2915 (1965).
32. S. I. Chan, T. R. Borgus, J. W. Russell, H. L. Strauss, and H. L. Gwinn, J. Chem. Phys., 44, 1103 (1966).
33. D. O. Harris, H. W. Harrington, A. C. Luntz, and W. D. Gwinn, J. Chem. Phys., 44, 3467 (1966); T. R. Borgers and H. L. Strauss, 45, 947 (1966).
34. L. A. Carreira and R. C. Lord, J. Chem. Phys., 51, 3225 (1969).
35. J. R. Durig, G. L. Coulter, and D. W. Wertz, J. Mol. Spectrosc., 27, 285 (1968).
36. J. Laane, J. Chem. Phys., 50, 1946 (1969).
37. D. W. Wertz, J. Chem. Phys., 51, 2133 (1969).
38. J. A. Greenhouse and H. L. Strauss, J. Chem. Phys., 50, 124 (1969).
39. G. C. Engerholm, A. C. Luntz, W. D. Gwinn and D. O. Harris, J. Chem. Phys., 50, 2446 (1969).
40. L. A. Carreira and R. C. Lord, J. Chem. Phys., 51, 2735 (1969).
41. J. Laane and R. C. Lord, J. Mol. Spectrosc., 39, 340 (1971).
42. R. C. Lord and T. B. Malloy, Jr., J. Mol. Spectrosc., 46, 358 (1973).
43. J. D. Lewis, J. Laane, and T. B. Malloy, Jr., J. Chem. Phys., 61, 2342 (1974).
44. W. Keifer, H. J. Bernstein, M. Danyluk, H. Wieser, Chem. Phys. Lett., 12, 605 (1972).
45. L. A. Carreira, G. J. Jiang, W. B. Person, and J. N. Willis, Jr., J. Chem. Phys., 56, 1440 (1972).
46. T. Ikeda and R. C. Lord, J. Chem. Phys., 56, 4450 (1972).
47. T. B. Malloy, Jr., J. Mol. Spectrosc., 44, 504 (1972).
48. J. Laane, J. Chem. Phys., 50, 1946 (1969).
49. J. R. Durig and J. N. Willis, J. Mol. Spectrosc., 32, 320 (1969).
50. J. R. Durig, W. J. Natter, and V. F. Kalasinsky, J. Chem. Phys., 67, 4756 (1977).
51. J. Wells, M. S. Thesis, Texas A&M University, 1983; J. Wells and J. Laane, to be published.

52. C. Cooper and J. Laane, to be published; C. Cooper, M. S. Thesis, Texas A&M University, 1986.
53. J. R. Villarreal and J. Laane, J. Chem. Phys., 68, 3298 (1978).
54. H. Oberhammer and S. H. Bauer, J. Amer. Chem. Soc., 91, 10 (1969).
55. L. A. Carreira, R. O. Carter, and J. R. Durig, J. Chem. Phys., 59, 812 (1973).
56. R. C. Lord and T. C. Rounds, J. Chem. Phys., 58, 4344 (1973).
57. R. C. Lord, T. C. Rounds, and T. Ueda, J. Chem. Phys., 57, 2572 (1972).
58. J. R. Durig, R. O. Carter, L. A. Carreira, J. Chem. Phys., 60, 3098 (1974).
59. L. A. Carreira, R. C. Lord, T. B. Malloy, Jr., Topics in Current Chemistry, Vol. 82, Springer-Verlag, Berlin, p. 3 (1979).
60. M. Tecklenburg and J. Laane, to be published.
61. V. E. Gaines and J. Laane, to be published.
62. J. Laane, J. R. Villarreal, and V. E. Gaines, unpublished results.
63. M. A. Harthcock, L. W. Richardson, and J. Laane, J. Phys. Chem., 88, 1365 (1984).
64. J. Laane, Quart. Rev., 25, 533 (1971).
65. C. S. Blackwell and R. C. Lord, Vibrational Spectra and Structure, J. R. Durig, ed., Vol. 1, Marcel Dekker, p. 1 (1972).
66. J. Laane, Vibrational Spectra and Structure, J. R. Durig, ed., Vol. 1, Marcel Dekker, p. 25 (1972).
67. T. B. Malloy, Jr., L. E. Bauman, and L. A. Carreira, Topics in Stereo-Chemistry, E. L. Eliel and N. L. Allinger (eds.), Vol. 14, Wiley Interscience, p. 97 (1979).
68. A. C. Legon, Chem. Rev., 80, 231 (1980).
69. J. Laane, J. Mol. Struct., 126, 99 (1985).
70. W. C. Harris and J. R. Durig, Vibrational Spectra and Structure, J. R. Durig, ed., Vol. 1, Marcel Dekker, p. 73 (1972).
71. J. R. Villarreal and J. Laane, J. Chem. Phys., 62, 303 (1975).
72. J. D. Lewis, T. B. Malloy, Jr., T. H. Chao, and J. Laane, J. Mol. Struct., 12, 427 (1972).
73. J. R. Durig, M. Zhen, and T. S. Little, J. Chem. Phys., 81, 4259 (1984).